

The Structures of Four Caesium Tellurates

BY B. O. LOOPSTRA AND K. GOUBITZ

Laboratory for Crystallography, University of Amsterdam, Nieuwe Achtergracht 166, 1018 WV Amsterdam, The Netherlands

(Received 15 October 1985; accepted 23 December 1985)

Abstract. (1) Cs_2TeO_3 , $M_r = 441.42$, $P321$, $a = 6.790$ (1), $c = 7.972$ (1) Å, $U = 318.3$ Å³, $Z = 2$, $D_x = 4.606$ g cm⁻³, Mo $K\alpha$, $\lambda = 0.71069$ Å, $\mu = 157.8$ cm⁻¹, $F(000) = 372$, room temperature, $R = 0.045$ for 415 unique reflections. (2) $\text{Cs}_2\text{Te}_2\text{O}_5$, $M_r = 601.02$, $Pbca$, $a = 12.102$ (1), $b = 12.092$ (2), $c = 10.760$ (2) Å, $U = 1574.6$ Å³, $Z = 8$, $D_x = 5.070$ g cm⁻³, Mo $K\alpha$, $\lambda = 0.71069$ Å, $\mu = 164.5$ cm⁻¹, $F(000) = 2032$, room temperature, $R = 0.060$ for 2592 unique reflections. (3) $\text{Cs}_2\text{Te}_4\text{O}_9$, $M_r = 920.21$, $I\bar{4}2d$, $a = 10.783$ (1), $c = 20.599$ (4) Å, $U = 2394.9$ Å³, $Z = 8$, $D_x = 5.104$ g cm⁻³, Mo $K\alpha$, $\lambda = 0.71069$ Å, $\mu = 156.6$ cm⁻¹, $F(000) = 3120$, room temperature, $R = 0.056$ for 1616 unique reflections. (4) $\text{Cs}_2\text{Te}_4\text{O}_{12}$, $M_r = 968.21$, $R\bar{3}m$, $a = 7.2921$ (4), $c = 18.332$ (2) Å, $U = 844.2$ Å³ [rhombohedral constants: $a = 7.4205$ (6) Å, $\alpha = 58.858$ (7)°, $U = 281.4$ Å³], $Z = 3$, $D_x = 5.713$ g cm⁻³, Mo $K\alpha$, $\lambda = 0.71069$ Å, $\mu = 166.8$ cm⁻¹, $F(000) = 1242$, room temperature, $R = 0.043$ for 622 unique reflections. Structures (1) and (2) are related to the perovskite structure, (3) and (4) are of the inverse pyrochlore type. In structures (1)–(3) Te^{IV} atoms are octahedrally coordinated by oxygens and holes, the number of holes varying from 1 to 3. In $\text{Cs}_2\text{Te}_4\text{O}_{12}$ the Te^{IV} atom is at the centre of a very nearly regular octahedron of oxygens, an exceptional coordination for tetravalent Te. In this octahedron the length of the Te–O bonds is 2.104 (7) Å.

Introduction. The elements caesium and tellurium play a prominent role in studies on the safety of nuclear reactors, owing to the formation of volatile compounds. For this reason the system Cs–Te–O was studied. All phases of the system TeO_2 – Cs_2TeO_3 , viz Cs_2TeO_3 , $\text{Cs}_2\text{Te}_2\text{O}_5$ and $\text{Cs}_2\text{Te}_4\text{O}_9$ (Cordfunke & Smit-Groen, 1984), were obtained in a suitable crystalline form. Furthermore, crystals of the mixed Te^{IV}–Te^{VI} oxide $\text{Cs}_2\text{Te}_4\text{O}_{12}$ were isolated. Attempts to isolate single crystals of Cs_2TeO_4 failed, and the same was true for the compounds intermediate between $\text{Cs}_2\text{Te}_4\text{O}_9$ and $\text{Cs}_2\text{Te}_4\text{O}_{12}$.

The crystal structures of the three tellurites and the mixed tellurite–tellurate mentioned above were investigated to gain some understanding of the relation-

ships between them. None of these structures has been described previously. The only caesium tellurate for which unit-cell data are known is Cs_2TeO_4 (Duquénoy, 1971).

Experimental. All specimens prepared by heating Cs_2CO_3 (Merck, 99.5% purity) and TeO_2 (BDH, 99.95% purity) in gold boats in an argon atmosphere for at least 15 h until X-ray pattern showed them to be pure. To obtain single crystals materials melted in gold boats under purified argon, followed by cooling at 2 K h⁻¹. Cooling ranges: Cs_2TeO_3 : 1103 to 953 K; $\text{Cs}_2\text{Te}_2\text{O}_5$: 723 to 673 K; $\text{Cs}_2\text{Te}_4\text{O}_9$: 848 to 788 K; $\text{Cs}_2\text{Te}_4\text{O}_{12}$: 913 to 873 K. After breaking melts specimen crystals were selected. $\text{Cs}_2\text{Te}_4\text{O}_{12}$ stable in air. All other specimens had to be sealed in glass capillaries in dry box.

Main experimental details are collected in Table 1. Nonius CAD-4 four-circle goniometer. Graphite-monochromated Mo $K\alpha$ radiation. Absorption correction by *DIFABS* (Walker & Stuart, 1983). Scattering factors from Cromer & Mann (1968), dispersion factors for Cs and Te from *International Tables for X-ray Crystallography* (1974). Cs and Te positions derived from Patterson functions, O positions from difference maps. Anisotropic temperature factors for Cs and Te, isotropic for O. Extinction correction applied for $\text{Cs}_2\text{Te}_2\text{O}_5$ and $\text{Cs}_2\text{Te}_4\text{O}_9$. Refinement based on block-diagonal least squares on F using *XRAY76* (Stewart, Machin, Dickinson, Ammon, Heck & Flack, 1976) and *XTAL* (Hall, Stewart & Munn, 1980). Equivalent reflections averaged after applying absorption correction to yield sets of unique reflections.

Discussion. Tables 2–5 list the final positional parameters for the four compounds. Stereoviews are given in Figs. 1–4. Bond lengths and angles are given in Table 6.*

* Lists of structure factors, anisotropic thermal parameters and full lists of bond lengths and angles have been deposited with the British Library Lending Division as Supplementary Publication No. SUP 42730 (95 pp.). Copies may be obtained through The Executive Secretary, International Union of Crystallography, 5 Abbey Square, Chester CH1 2HU, England.

The structures of Cs_2TeO_3 and $\text{Cs}_2\text{Te}_2\text{O}_5$ are related to perovskite ABO_3 . This is most easily seen in the case of $\text{Cs}_2\text{Te}_2\text{O}_5$, which can be described as $\text{Cs}_2\text{Te}_2\text{O}_5 + \square$, the \square representing a hole occupied by the free-electron pairs of the two Te atoms. $\text{Cs}_2\text{Te}_2\text{O}_5$ is also closely related to cryolite Na_3AlF_6 (Naráy-Szabó & Sasvári, 1938). Te atoms are octahedrally coordinated by three bonded oxygens, two non-bonded oxygens and a hole. Two Te atoms share an oxygen to form Te_2O_5 groups. Two Te_2O_5 groups join holes to accommodate their free electrons.

Table 1. *Experimental data for (1) to (4)*

	Cs_2TeO_3	$\text{Cs}_2\text{Te}_2\text{O}_5$	$\text{Cs}_3\text{Te}_4\text{O}_9$	$\text{Cs}_5\text{Te}_6\text{O}_{12}$
Crystal size (mm)	0.2 × 0.1 × 0.05	0.5 × 0.2 × 0.1	0.3 × 0.2 × 0.1	0.1 × 0.06 × 0.03
Reflections for measuring lattice parameters, $\theta_{\text{max}}(^{\circ})$	24, 22	24, 18	24, 22	23, 39
$\theta_{\text{max}}(^{\circ})$	35	37	40	40
Min. h, k, l	0, 0, -12	0, 0, -18	-9, -9, 0	0, 0, -33
Max. h, k, l	21, 21, 12	20, 20, 18	9, 9, 12	11, 11, 33
Reflections measured	1110	8530	4025	1354
Reflections with $I > 2.5\sigma(I)$	744	4003	2565	1068
Unique observed reflections	415	2592	1616	622
Control reflection	220	184	488	113
		284		
Intensity variation of control reflection (%)	±7.8	±3.4	±6.8	±3.3
$(\Delta\rho)_{\text{max.}}$ ($\text{e } \text{Å}^{-3}$)	1.8	3.6	3.0	3.7
$(\Delta\rho)_{\text{min.}}$ ($\text{e } \text{Å}^{-3}$)	-1.8	-4.2	-3.0	-9.8
R_{int}	0.045	0.060	0.056	0.043
$(I/\sigma)_{\text{max.}}$	0.05	0.37	0.56	0.0
Absorption correction				
max.	1.41	1.43	1.45	1.60
min.	0.77	0.66	0.81	0.81
Extinction correction	—	0.1	0.4	—

Table 2. *Positional parameters and U_{eq} values ($\text{Å}^2 \times 100$, $U_{\text{eq}} = \frac{1}{3} \sum U_{ii}$) with e.s.d.'s for Cs_2TeO_3*

	x	y	z	U_{eq}
Cs(1)	0.0	0.0	0.0	2.55 (6)
Cs(2)	0.0	0.0	0.5	2.33 (5)
Cs(3)	0.3333	0.6667	0.3589 (2)	3.19 (5)
Te	0.6667	0.3333	0.1644 (1)	1.74 (3)
O	0.837 (3)	0.611 (2)	0.269 (1)	4.66 (34)

Table 3. *Positional parameters and U_{eq} values ($\text{Å}^2 \times 100$, $U_{\text{eq}} = \frac{1}{3} \sum U_{ii}$) with e.s.d.'s for $\text{Cs}_2\text{Te}_2\text{O}_5$*

	x	y	z	U_{eq}
Cs(1)	0.24742 (6)	0.24601 (6)	0.24745 (7)	1.79 (2)
Cs(2)	0.49552 (6)	0.49488 (6)	0.21370 (6)	1.69 (2)
Te(1)	0.26329 (5)	0.00935 (5)	-0.00048 (7)	1.26 (2)
Te(2)	0.48853 (5)	0.23672 (5)	0.00289 (7)	1.26 (2)
O(1)	0.4980 (7)	0.2267 (7)	0.1730 (8)	1.93 (15)
O(2)	0.1534 (8)	0.1130 (8)	-0.0106 (10)	2.44 (17)
O(3)	0.2744 (8)	-0.0078 (9)	0.1690 (10)	2.58 (18)
O(4)	0.3857 (8)	0.3464 (8)	-0.0148 (9)	2.24 (16)
O(5)	0.3913 (9)	0.1089 (9)	-0.0280 (10)	2.73 (19)

Table 4. *Positional parameters and U_{eq} values ($\text{Å}^2 \times 100$, $U_{\text{eq}} = \frac{1}{3} \sum U_{ii}$) with e.s.d.'s for $\text{Cs}_2\text{Te}_4\text{O}_9$*

	x	y	z	U_{eq}
Cs(1)	0.7205 (2)	0.25	0.125	3.62 (9)
Cs(2)	0.0	0.5	0.00586 (8)	2.54 (6)
Te(1)	0.1250 (1)	0.1214 (1)	0.06183 (4)	1.61 (3)
Te(2)	0.3655 (1)	0.3905 (1)	0.07226 (4)	1.50 (3)
O(1)	0.297 (1)	0.506 (2)	0.0170 (6)	2.81 (25)
O(2)	0.171 (1)	0.069 (1)	-0.0213 (6)	2.30 (22)
O(3)	0.172 (1)	0.286 (1)	0.0533 (6)	2.45 (23)
O(4)	0.286 (1)	0.054 (1)	0.0975 (6)	2.34 (23)
O(5)	0.5	0.5	0.1035 (8)	2.21 (29)

Table 5. *Positional parameters and U_{eq} values ($\text{Å}^2 \times 100$, $U_{\text{eq}} = \frac{1}{3} \sum U_{ii}$) with e.s.d.'s for $\text{Cs}_2\text{Te}_4\text{O}_{12}$*

	x	y	z	U_{eq}
Cs	0.0	0.0	0.12200 (7)	1.62 (3)
Te(1)	0.0	0.0	0.5	0.35 (3)
Te(2)	0.5	0.0	0.0	0.20 (2)
O(1)	0.2036 (6)	-0.2036 (6)	-0.0172 (4)	1.01 (10)
O(2)	0.1364 (6)	-0.1364 (6)	0.4341 (4)	0.95 (10)

Table 6. *Bond lengths (Å) and angles (°) around Te atoms*

(1) Cs_2TeO_3			
Te—O (3×)	1.84 (2)	O—Te—O ⁱ	101 (1)
(2) $\text{Cs}_2\text{Te}_2\text{O}_5$			
Te(1)—O(2)	1.83 (1)	O(2)—Te(1)—O(3)	100.9 (5)
—O(3)	1.84 (1)	O(2)—Te(1)—O(5)	98.2 (4)
—O(5)	1.98 (1)	O(3)—Te(1)—O(5)	99.2 (4)
Te(2)—O(4)	1.83 (1)	O(1)—Te(2)—O(4)	101.2 (4)
—O(1)	1.84 (1)	O(1)—Te(2)—O(5)	98.8 (4)
—O(5)	1.97 (1)	O(4)—Te(2)—O(5)	98.3 (4)
(3) $\text{Cs}_3\text{Te}_4\text{O}_9$			
Te(1)—O(3)	1.86 (1)	O(3)—Te(1)—O(2)	97.6 (6)
—O(2)	1.87 (1)	O(3)—Te(1)—O(4)	98.1 (6)
—O(4)	2.02 (1)	O(3)—Te(1)—O(2 _i)	89.6 (5)
—O(2 _{ii})	2.31 (1)	O(2)—Te(1)—O(4)	89.9 (6)
		O(2)—Te(1)—O(2 _i)	88.7 (5)
		O(4)—Te(1)—O(2 _i)	172.3 (5)
Te(2)—O(1)	1.84 (2)	O(1)—Te(2)—O(4 _i)	98.1 (6)
—O(4 _{ii})	1.96 (1)	O(1)—Te(2)—O(5)	95.1 (6)
—O(5)	1.98 (1)	O(1)—Te(2)—O(3)	82.5 (6)
—O(3)	2.40 (1)	O(1)—Te(2)—O(1 _i)	92.2 (5)
—O(1 _{ii})	2.51 (1)	O(4 _i)—Te(2)—O(5)	82.3 (6)
		O(4 _i)—Te(2)—O(3)	84.2 (5)
		O(4 _i)—Te(2)—O(1 _i)	169.3 (5)
		O(5)—Te(2)—O(3)	165.8 (4)
		O(5)—Te(2)—O(1 _i)	94.2 (5)
		O(3)—Te(2)—O(1 _i)	99.9 (5)
(4) $\text{Cs}_5\text{Te}_6\text{O}_{12}$			
Te(1)—O(2)	(6×) 2.104 (7)	O(2)—Te(1)—O(2 _{ii})	89.7 (2)
Te(2)—O(2 _i)	(2×) 1.886 (6)	O(1)—Te(2)—O(1 _{ii})	86.0 (2)
—O(1)	(4×) 1.941 (6)	O(1)—Te(2)—O(2 _i)	88.6 (3)

Symmetry code: (i) $1-y, x-y, z$; (ii) $-y, x, -z$; (iii) $x, \frac{1}{2}-y, \frac{1}{2}-z$; (iv) $1-y, x, -z$; (v) $\frac{2}{3}-x, \frac{1}{3}-2x, \frac{1}{3}-z$; (vi) $2x, x, 1-z$; (vii) $2x, x, -z$.

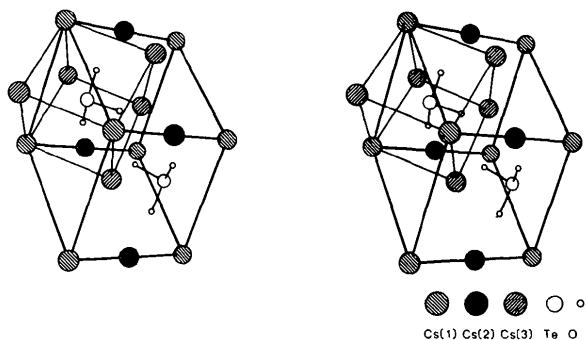


Fig. 1. Cs_2TeO_3 . Outlines of unit cell (heavy) and subcell (light) are drawn.

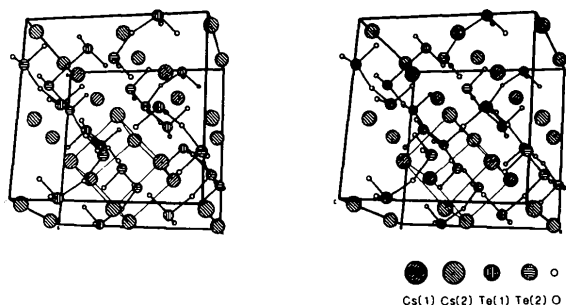


Fig. 2. $\text{Cs}_2\text{Te}_2\text{O}_5$. Outlines of unit cell (heavy) and subcell (light) are drawn.

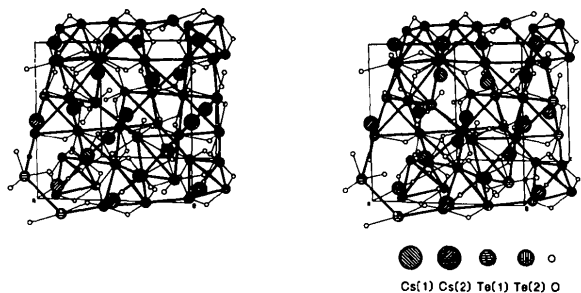


Fig. 3. $\text{Cs}_2\text{Te}_4\text{O}_9$. For clarity only the part from $z = -0.05$ to $z = 0.65$ is drawn. To show the correspondence with $\text{Cs}_2\text{Te}_4\text{O}_{12}$ the Te-Te tetrahedra are indicated by a heavy outline.

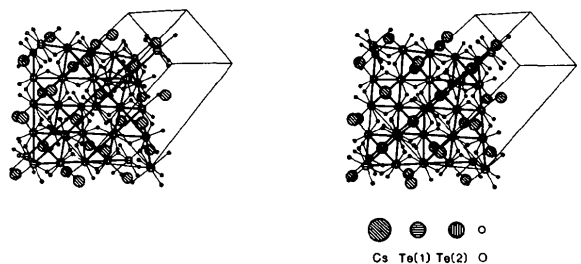


Fig. 4. $\text{Cs}_2\text{Te}_4\text{O}_{12}$. The contents of the pseudo-cubic F cell and the edges of the hexagonal cell are shown. Te-Te tetrahedra are indicated by a heavy outline.

In Cs_2TeO_3 , two formula units occupy three rhombohedral perovskite subcells of dimension $a = 4.736 \text{ \AA}$, $\alpha = 91.59^\circ$: $A_3B_3O_9 \rightarrow \text{Cs}_3(\text{CsTe}_2)\text{O}_6$. Cs(2) and Te occupy octahedral B positions, Cs(1) and Cs(3) A positions. Because, compared to perovskite, $1/3$ of the oxygen sites are empty, the twelve coordination of the A positions is reduced to nine for Cs(3) and six for Cs(1). Te free-electron pairs combine to form channels. The TeO_3^{2-} groups do not share oxygens. Te is octahedrally bonded to and coordinated by three oxygens; the remaining positions around the Te site are empty. Powder patterns of Cs_2TeO_3 show a doubling of the a axis, giving rise to a number of weak reflections (Cordfunke & Van Vlaanderen, 1985). These reflections were not observed in the present study. Clearly, the true structure is somewhat more complicated than the one derived from our data.

$\text{Cs}_2\text{Te}_4\text{O}_9$ and $\text{Cs}_2\text{Te}_4\text{O}_{12}$ are closely related. $\text{Cs}_2\text{Te}_4\text{O}_{12}$, the simplest of the two, is isostructural with the inverse pyrochlores (Babel, Pausewang & Viebahn, 1967) and resembles $\text{Cs}_2\text{U}_4\text{O}_{12}$ (Van Egmond, 1975). This latter compound exists in a trigonal form ($R\bar{3}m$, $a = 10.962 \text{ \AA}$, $\alpha = 89.40^\circ$) as well as in a closely related monoclinic and a cubic one ($Fd\bar{3}m$, $a = 11.2295 \text{ \AA}$). Likewise, $\text{Cs}_2\text{Te}_4\text{O}_{12}$ can be described by a near-cubic rhombohedral cell ($a = 10.383 \text{ \AA}$, $\alpha = 88.99^\circ$). Its positions are seen to approximate the inverse pyrochlore positions in $Fd\bar{3}m$ closely after transformation by $-\frac{1}{2}, 0, 1$; $\frac{1}{2}, -\frac{1}{2}, 1$; $0, \frac{1}{2}, 1$ (origin at centre of symmetry). Result: Cs \sim at $8(a)$ ($0.122, 0.122, 0.122$), Te \sim at $16(d)$, O \sim at $48(f)$ ($0.433 \pm 0.004, 0.125 \pm 0.007, 0.125 \pm 0.007$). Te(1) and Te(2) transform into one cubic position, O(1) and O(2) very nearly do so (the \pm values show the deviations from the average position). For the cubic form of $\text{Cs}_2\text{U}_4\text{O}_{12}$, the only one for which the oxygen coordinates are quoted (Van Egmond, 1975), the structure determination based on high-temperature powder work indicates $x(\text{O}) = 0.449$ (5).

In $\text{Cs}_2\text{Te}_4\text{O}_9$, two pseudo-cubic cells are stacked leading to the doubling of the c axis of the unit cell. If only metal sites are considered, $\text{Cs}_2\text{Te}_4\text{O}_{12}$ and $\text{Cs}_2\text{Te}_4\text{O}_9$ are isostructural with each other and with Cu_2Mg . Te atoms are situated at the corners of tetrahedra linked to each other to form a three-dimensional network with large holes occupied by the Cs atoms. In $\text{Cs}_2\text{Te}_4\text{O}_{12}$ all Te-Te edges of each tetrahedron carry an oxygen, resulting in truly octahedral tellurate groups. In $\text{Cs}_2\text{Te}_4\text{O}_9$, one out of four tetrahedra carries six oxygens, the others have four. This results in octahedral Te-O groups with one or two holes: Te(1) is bonded to four O atoms and Te(2) to five, including weak bonds up to 2.51 \AA (Table 6).

It is remarkable that in $\text{Cs}_2\text{Te}_4\text{O}_{12}$ both Te^{IV} and Te^{VI} have a quite regular octahedral oxygen coordination. Whereas this is usual for Te^{VI} , Te^{IV} appears normally in a deformed and incomplete octahedral coordination

with a coordination number, including all oxygens at less than 3 Å, ranging from 3 to 5, and a number of bonds up to and often less than five. To the accuracy of the present data, Te(1) is situated at a centre of symmetry with six equivalent Te^{IV}-O bonds of 2.104 (7) Å and angles of 90 ± 0.5°. There is no indication, for example from the temperature factor, that Te(1) is at a site of too high symmetry, to be lowered by changing the space group from *R*3̄*m* to *R*3*m*. In fact, refining in *R*3*m* does not change the Te coordination to any significant extent, as would also hardly be conceivable for a near-cubic structure.

The authors are indebted to Professor Dr E. H. P. Cordfunke and Mr P. Van Vlaanderen of the Netherlands Energy Research Foundation ECN for preparation of the specimens and their great interest shown in the work, and to Mr D. Heijdenrijk for his untiring efforts to select samples and collect the X-ray data.

Acta Cryst. (1986). **C42**, 523–525

Redetermination of Tricalcium Uranate(VI). A Rietveld Refinement of Neutron Powder Diffraction Data

BY H. C. VAN DUIVENBODEN AND D. J. W. IJDO

Gorlaeus Laboratories, State University, Leiden, PO Box 9502, 2300 RA Leiden, The Netherlands

(Received 11 September 1985; accepted 24 December 1985)

Abstract. Ca₃UO₆, *M_r* = 454.27, monoclinic, *P*2₁/*n*, *Z* = 2. At room temperature: *a* = 5.7292 (7), *b* = 5.9562 (7), *c* = 8.2991 (10) Å, β = 90.56 (1)°, *V* = 283.19 (6) Å³, *D_x* = 5.327 (1) Mg m⁻³, μ*R* = 0.14. The structure has been refined by Rietveld analysis of powder neutron diffraction data [λ = 2.5790 (3) Å, *R_{wp}* = 6.14%] for 136 reflections. The structure is of monoclinic, deformed CaTiO₃ type, with ordering of Ca and U in octahedral positions. The stability in water at 573 K and 0.2 GPa for 1 week was tested: it was found that Ca₃UO₆ is totally decomposed under these conditions.

Introduction. The preparation, crystal structure determination and solubility test in water at elevated temperatures and pressures form part of a research program to investigate compounds with perovskite or related structures for their properties as a host lattice for nuclear waste. Ca₃UO₆ is reported to adopt a monoclinic, deformed perovskite-like structure with space group *P*2₁ (Loopstra & Rietveld, 1969). In relation to other substituted perovskites this space group seems too low. The powder diffraction data

References

- BABEL, D., PAUSEWANG, G. & VIEBAHN, W. (1967). *Z. Naturforsch. Teil B*, **22**, 1219–1220.
 CORDFUNKE, E. H. P. & SMIT-GROEN, V. M. (1984). *Thermochim. Acta*, **80**, 181–183.
 CORDFUNKE, E. H. P. & VAN VLAANDEREN, P. (1985). Private communication.
 CROMER, D. T. & MANN, J. B. (1968). *Acta Cryst.* **A24**, 321–324.
 DUQUÉNOY, G. (1971). *Rev. Chim. Minér.* **8**, 683–721.
 HALL, S. R., STEWART, J. M. & MUNN, R. J. (1980). *Acta Cryst.* **A36**, 979–989.
International Tables for X-ray Crystallography (1974). Vol. IV. Birmingham: Kynoch Press. (Present distributor D. Reidel, Dordrecht.)
 NARÁY-SZABÓ, S. & SASVÁRI, K. (1938). *Z. Kristallogr.* **99A**, 27–31.
 STEWART, J. M., MACHIN, P. A., DICKINSON, C. W., AMMON, H. L., HECK, H. & FLACK, H. (1976). The XRAY76 system. Tech. Rep. TR-446. Computer Science Center, Univ. of Maryland, College Park, Maryland.
 VAN EGMOND, A. B. (1975). *J. Inorg. Nucl. Chem.* **37**, 1929–1931.
 WALKER, N. & STUART, D. (1983). *Acta Cryst.* **A39**, 158–166.

suggest the space group *P*2₁/*n* in agreement with the powder diffraction data of Ca₃WO₆ (JCPDS file No. 22–541).

Experimental. AR starting materials CaCO₃ and U₃O₈ thoroughly mixed in an agate mortar in the appropriate ratio; mixture heated in a platinum crucible at 1073 K for 1 d and, after grinding, heated at 1473 K for one week with repeated grindings, and annealed one week at 1073 K.

X-ray powder diffraction pattern obtained with a Philips PW 1050 diffractometer; all lines could be indexed with a monoclinic unit cell, in accordance with electron diffraction data (Siemens Elmiskop 102 electron microscope, double tilt, lift cartridge, 100 kV). Lattice absences *h*0*l* *h*+*l*=2*n*+1 and 0*k*0 *k*=2*n*+1 in accordance with space group *P*2₁/*n*. Since no single crystals were available, Rietveld's (1969) method was used for refinement of neutron powder diffraction data; neutron powder profile recorded (room temperature, atmospheric pressure) at the Petten High-Flux Reactor; 5° < 2θ < 163° in steps of 0.1°; neutrons at room temperature from (111) planes of a Cu crystal;